Psychopharmacology (2018) 235:1257–1271
https://doi.org/10.1007/s00213-018-4841-8

ORIGINAL INVESTIGATION

Mapping brain functional alterations in betel-quid chewers using resting-state fMRI and network analysis

Jun-Cheng Weng[1,2] · Yu-Syuan Chou[3] · Guo-Joe Huang[4] · Yeu-Sheng Tyan[3,5] · Ming-Chou Ho[4,6]

Received: 7 September 2017 / Accepted: 21 January 2018 / Published online: 13 February 2018

Abstract

Rationale The World Health Organization regards betel quid (BQ) as a human carcinogen, and DSM-IV and ICD-10 dependence symptoms may develop with its heavy use. BQ's possible effects of an enhanced reward system and disrupted inhibitory control may increase the likelihood of habitual substance use.

Objectives The current study aimed to employ resting-state fMRI to examine the hypothesized enhanced reward system (e.g., the basal forebrain system) and disrupted inhibitory control (e.g., the prefrontal system) in BQ chewers.

Methods The current study recruited three groups of 48 male participants: 16 BQ chewers, 15 tobacco- and alcohol-user controls, and 17 healthy controls. We used functional connectivity (FC), mean fractional amplitude of low-frequency fluctuations (mfALFF), and mean regional homogeneity (mReHo) to evaluate functional alternations in BQ chewers. Graph theoretical analysis (GTA) and network-based statistical (NBS) analysis were also performed to identify the functional network differences among the three groups.

Results Our hypothesis was partially supported: the enhanced reward system for the BQ chewers (e.g., habitual drug-seeking behavior) was supported; however, their inhibitory control was relatively preserved. In addition, we reported that the BQ chewers may have enhanced visuospatial processing and decreased local segregation.

Conclusions The current results (showing an enhanced reward system in the chewers) provided the clinicians with important insight for the future development of an effective abstinence treatment.

Keywords Betel quid · Resting-state functional MRI (rs-fMRI) · Functional connectome · Graph theoretical analysis (GTA) · Network-based statistical (NBS) analysis

✉ Ming-Chou Ho
mingchou@csmu.edu.tw; mcho1976@ntu.edu.tw

[1] Department of Medical Imaging and Radiological Sciences, Chang Gung University, Taoyuan, Taiwan

[2] Department of Psychiatry, Chang Gung Memorial Hospital, Chiayi, Taiwan

[3] Department of Medical Imaging and Radiological Sciences, Chung Shan Medical University, Taichung, Taiwan

[4] Department of Psychology, Chung Shan Medical University, No. 110, Sec. 1, Chien-Kuo N. Road, Taichung 402, Taiwan

[5] Department of Medical Imaging, Chung Shan Medical University Hospital, Taichung, Taiwan

[6] Clinical Psychological Room, Chung Shan Medical University Hospital, Taichung, Taiwan

Introduction

Betel quid (BQ; "bin lang" in Taiwanese Mandarin) is the fourth most commonly used drug worldwide, after tobacco, alcohol, and caffeine (Winstock 2002). The World Health Organization regards BQ as a human carcinogen (IARC 2004), and DSM-IV and ICD-10 dependence symptoms may develop with heavy use (Benegal et al. 2008; Lee et al. 2014). The Ministry of Health and Welfare reported some 15.8% male chewers and 1.0% female chewers among the population of Taiwan (MHW 2008). Chewers place a whole BQ into their mouths and macerate it by biting for approximately 2–3 min; they then spit out the saliva, which has turned red from chewing the BQ. However, the limited understanding of chronic BQ chewing makes it difficult for development of effective treatment (Osborne et al. 2017).

In this study, we used resting-state functional magnetic resonance imaging (rs-fMRI) to examine the brain's functional alterations in BQ chewers. Recently, Chen et al. (2015) reported the first structural imaging, suggesting that BQ chewers exhibited a decrease in gray matter (GM) volume in the midbrain, the right anterior cingulate cortex (ACC), the bilateral dorsolateral prefrontal cortex (dlPFC), and the right superior temporal gyrus (STG), and an increased volume in the right hippocampus and the right precuneus. Liu et al. (2015) reported brain biochemical alterations (e.g., lower N-acetyl-aspartate/creatine) in the ACC in the BQ chewers, revealing possible impaired control abilities. Using resting-state fMRI (rs-fMRI), Liu et al. (2016a) found that the BQ chewers had increased functional connectivity (FC) from the ACC to the reward network and decreased connectivity from the ACC to the default mode network (DMN). Liu et al. (2016c) reported that the BQ chewers had alternations in the distant and local FC densities primarily in the brain areas involved in the DMN (e.g., right rostral ACC and bilateral inferior parietal lobule) and inhibitory control (right ACC and dorsolateral prefrontal cortex (dlPFC)). Another rs-fMRI study (Liu et al. 2016b) found decreased ALFF and ReHo in the PFC in BQ chewers. Huang et al. (2016) reported that for the non-chewers, chewing BQ can immediately increase the FC of the frontal networks (e.g., the orbital frontal and frontoparietal networks) and decrease that of the DMN. In BQ chewers, Huang et al. (2017) found increased FC in the networks (e.g., the orbital frontal network) related to reward sensitivity and affective decision-making and decreased FC in the networks (e.g., medial frontal/anterior cingulate network) parts of DMN. Zhu et al. (2017) reported disrupted FC within the DMN in the BQ chewers. Yuan et al. (2017) revealed structural differences between the BQ chewers and non-chewers, particularly in the areas involved in inhibitory control (e.g., *dlPFC*) and affective decision-making (e.g., ventral medial prefrontal cortex (*vmPFC*)).

By using generalized q-sampling imaging (GQI), Weng et al. (2017) reported that the BQ chewers might not have disrupted inhibitory control (e.g., the increased diffusion anisotropy in the right ACC). They also reported an enhanced basal forebrain reward system in the BQ chewers. In sum, the recent BQ imaging studies consistently showed a hyperactive basal forebrain reward system and overvalued the reinforcement effect of BQ on the chewers.

Functional magnetic resonance imaging (fMRI), based on the blood oxygenation level-dependent (BOLD) effect to measure brain activity, provides an opportunity to refine pathoetiological models of chewing BQ. The use of rs-fMRI simplifies and facilitates the examination of brain activity during the resting status of the participant with highly standardized and reproducible procedures and without any task-requirement (Biswal et al. 1995; Greicius et al. 2003; Raichle et al. 2001). Therefore, rs-fMRI has attracted the attention of interested researchers and its use has widened in clinical applications. The amplitude of low-frequency fluctuation (ALFF) is used to approximate the absolute intensity of spontaneous brain activity. These spontaneous low-frequency fluctuations have numerous similarities with fluctuations in the neural metabolic, hemodynamic, and neurophysiological parameters (Zhang et al. 2014). The ALFF during the resting state is considered to be physiologically meaningful and reflective of spontaneous neural activity (Yue et al. 2015). Regional homogeneity (ReHo) is based on the concept that BOLD signal fluctuations in a specific region reflect near-neuronal activity arising at the same frequency and that this temporal synchrony is confined to groups of neurons performing related functions (Philip et al. 2013).

The functional connectome has recently been proposed as a conceptual framework for brain research (Bullmore and Bassett 2011; Chen et al. 2016; Gong and He 2015; Lo et al. 2011; Zhang et al. 2011). Tacit to this model is the functional organization of the human brain into complex networks, allowing for the segregation and integration of information processing. Based on topology, graph theoretical analysis quantitatively provides novel insight into the functional connectome by using nodes, edges, and several additional topological parameters, such as clustering coefficient, characteristic path length, and small-worldness (Bullmore and Sporns 2009; Hosseini et al. 2012).

In the current study, we examined the functional alternations in the BQ chewers by using rs-fMRI and network analysis. The recent rs-fMRI studies on BQ chewers (Liu et al. 2016a, b) suggested enhanced reward system (e.g., the basal forebrain system) and disrupted inhibitory control (e.g., the prefrontal system and the ACC); therefore, we hypothesized that these functional alternations may be observed, in terms of the following rs-fMRI indexes. The FC provides the time-based BOLD-signal correlations within the brain regions. The ALFF and ReHo provide information regarding the regional properties of brain activity during the resting state. Graph theoretical analysis (GTA) and network-based statistical (NBS) analysis provide network-based information for a more comprehensive understanding of the functional brain network in BQ chewers.

Recently, (Liu et al. 2016a, b) have employed some of these indexes (FC, ALFF, and ReHo) in their studies. These indexes are commonly adopted in the studies using rs-fMRI. In addition, the adoption of these indexes is necessary in the current study for at least two reasons. First, the preparation of BQ in China (Liu et al. 2016a, b) and Taiwan (the current study) may differ (Lee et al. 2014; Osborne et al. 2017) and may somehow affect chewers' brains to different extent. For example, in China (except Hainan), the BQ was prepared with dried husk of the areca fruit rather than the unripe areca fruit in Taiwan. In addition, in Taiwan, the betel leaf and the betel inflorescence

are the common additives. Second, the Taiwanese BQ chewers are usually cigarette smokers and alcoholic beverage drinkers (Ho 2014; Ko et al. 1992; Wen et al. 2005). The effect of the concurrent usage of cigarette and alcohol was assessed in the current study.

Methods and materials

Participants

The current study recruited three groups of 48 male participants: 16 BQ chewers (age 22–62 years, mean = 37.13 years, SD = 10.44 years), 15 tobacco- and alcohol-user controls (hereafter, TA controls) (age 23–41 years, mean = 30.07 years, SD = 4.88 years), and 17 healthy controls (hereafter, HC) (age 24–37 years, mean = 31.59 years, SD = 3.61 years). All participants were at least 20 years of age and right-handed. The participants were recruited via three methods: human resources or employment agencies, recruitment advertisements, and introduction by former participants.

The inclusion criteria for the BQ chewers were (a) current status as BQ chewers, and (b) dependence scores higher than the cut-off point of 24 on the Betel Nut Dependency Scale (BNDS) (Li et al. 2012). The BNDS consists of three factors: craving and desire (four items; e.g., if possible, I would like to chew BQ right now), withdrawal response (four items; e.g., when BQ is not available, I feel so upset that my work and activities are disturbed), and tasting habits (three items; e.g., I care about types, textures, and the feeling that comes from chewing BQ). Higher scores (range 11 to 44) indicate a higher level of dependence on BQ chewing. The three factors accounted for 63.10% of total variances, and α coefficients of reliability were between 0.73 and 0.89. Most of the model-fit indexes showed good fitting results (RMSEA = 0.070, SRMR = 0.038, AGFI = 0.90, GFI = 0.94, NFI = 0.97, NNFI = 0.98, CFI = 0.98, IFI = 0.98, RFI = 0.96), suggesting optimal construct validity of the scale. The scale also had good criterion-related validity. For example, the BNDS score correlated positively to the number of days per week on which chewing occurred and the average number of BQ chewed per day. The BNDS score correlated negatively to the extent of willing to quit chewing BQ. The TA controls were included if they had never chewed BQ and if they were current cigarette and alcohol users. The HC were included if they had never used BQ, cigarettes, or alcohol.

All participants signed the informed consent, approved by the Institutional Review Board of Chung-Shan Medical University Hospital. All participants completed the BNDS (Li et al. 2012), the Fagerstrom Test for Nicotine Dependence (FTND) (Fagerström 1978; Huang et al. 2006), and the Alcohol Use Disorders Identification Test (AUDIT) (Chen et al. 2005; Saunders et al. 1993).

Exclusion criteria for all participants were any eye diseases (e.g., cataract and glaucoma), history of another primary mental disorder (e.g., schizophrenia) or alcohol/illicit-substance-use disorder during the past year, any neurological illnesses, the current taking of any prescription or psychotropic medications, and metallic implants or other contraindications on the MRI.

Participants with a family history of substance-use disorders were ruled out. It was critical to rule out these participants, particularly when comparing the HC versus the substance-use group (Ersche et al. 2012, 2013). The HC with a family history of substance-use disorders might have brain abnormalities similar to those in the substance-use groups, possibly due to genetic or epigenetic influences (Ersche et al. 2012, 2013).

MRI data acquisition

All participants were scanned using a 3-T MRI (Skyra, Siemens, Germany) imaging system with an echo planar image (EPI) sequence to obtain resting-state functional images. All subjects were asked to relax, close their eyes, and not think of anything, although they could not fall asleep when the resting-state fMRI was performed. The parameters of the images were: TR/TE = 2000/30 ms, field of view (FOV) = 250 mm × 250 mm, matrix size = 94 × 94, in-plane resolution (pixel size) = 2.7 × 2.7 mm^2, thickness = 4 mm, number of repetitions = 240, and 28 axial slices aligned along AC-PC lines without gap to cover the whole cerebrum.

Functional image preprocessing

Preprocessing was conducted using statistical parametric mapping 8 (SPM8, Wellcome Department of Cognitive Neurology, London, UK) software. After slice-timing correction, we calculated the center of each image and realigned the data to the first volume for motion correction (if the result of six head motion parameters exceeded 1 mm translation or 1° rotation, it was excluded from this study). All of the participants fitted the criteria and no one was excluded. Following motion correction, data were normalized to standard Montreal Neurological Institute (MNI) space with affine transform and the data were resampled to isotropic 3-mm voxels. The data were then spatially smoothed using a 6-mm full width at half maximum (FWHM) Gaussian kernel for a better signal-to-noise ratio gain. Nuisance regression was then performed using the six head motion parameters as covariates. Then, the whole brain, WM, and CSF masks were used to remove the physiological noise. Linear detrending and band-pass temporal filtering were performed on the time series of each voxel to minimize the effects of low-frequency drifts and physiological signals by the Resting-State Data Analysis tool kit v1.8 (REST v1.8, Center for Cognition and Brain Disorders,

Hangzhou Normal University, Zhejiang, China). Previous studies suggested that the frequencies with important physiological information were in the range of 0.01–0.08 Hz (Cordes et al. 2001; Raichle et al. 2001). However, some research suggests that complex functional networks may be observed in the range of 0.1–0.12 Hz (Baria et al. 2011). Therefore, we extended the frequency range from 0.01 to 0.12 Hz to mitigate the influence of low-frequency drift and high-frequency physiological noise.

Functional connectivity and seed-based correlation analysis

As spontaneous, coherent, and low-frequency fluctuations of the BOLD-signal were used for the resting-state analysis, the BOLD time series for each participant was extracted and band-pass-filtered (0.01–0.12 Hz). Correlation maps at the voxel level were constructed by correlating the averaged BOLD signal of the user-defined region of interest to the BOLD signal of every other single voxel for each participant. To enforce a Gaussian distribution of the correlation data, the Pearson's correlation r was then transformed into z scores using the Fisher's r to z transformation. After seed-based correlation analysis (SCA), we averaged the threshold FC map of each individual with the same seed from the control group as the standard. Then we followed the standard FC map of each seed to draw the opposite side using the ROIs to calculate the correlation between bilateral seeds by image processing and analysis with ImageJ (National Institutes of Health, Bethesda, MD, USA). Finally, we averaged the three sections of each seed with the strongest signals to quantify the correlation between the bilateral seeds.

Amplitude of low-frequency fluctuations

The ALFF was calculated in the frequency range of 0.01 to 0.12 Hz. The procedure for calculating ALFF is briefly described as follows: for a given voxel, the time series was first converted to the frequency domain using a Fast Fourier Transform. The square root of the power spectrum was computed, averaged, and normalized across a predefined frequency interval, which was termed the ALFF at the given voxel (Yue et al. 2015). The mean fractional ALFF (mfALFF) can be regarded as a normalized mean ALFF and is calculated using the total energy over the detectable frequency range. The mfALFF can provide a more specific measure of low-frequency oscillatory phenomena than mALFF (Zou et al. 2008). We then performed two-sample t tests with false discovery rate (FDR) correction to assess the difference in mfALFF between the BQ chewers and the healthy controls. In addition, age and years of education were used as the covariates. To view the results, we used a T1-weighted MNI template to create the underlying map.

Regional homogeneity

To analyze ReHo, linear detrending and band-pass filtering (0.01–0.12 Hz) were performed on the time series of each voxel by REST v1.8. The ReHo approach was used to evaluate the resting state cortical activity in the BQ chewers and the healthy controls. Each individual ReHo map was generated by calculating the Kendall's coefficient of concordance (KCC), which computes the ReHo of the BOLD time series data in each voxel and its 26 nearest adjacent voxels (Zang et al. 2004). A mask was then used to remove non-brain tissues and noise on the ReHo maps, and the individual ReHo maps were divided by their own mean KCC within the mask for standardization purposes to compute the mean ReHo (mReHo). To evaluate group differences in mReHo between the BQ chewers and the healthy controls, we conducted a whole-brain voxel-wise comparison using two-sample t tests with FDR correction. Age and years of education were used as the covariates. To view the results, we used a T1-weighted MNI template to create the underlying map.

Graph theoretical analysis

In GTA, we first defined a set of nodes and edges. Using the functional connectivity toolbox (CONN, the Gabrieli Lab., McGovern Institute for Brain Research, MIT, USA), the whole brain was divided into 90 regions of interest (ROIs) (45 per hemisphere) with an automated anatomical labeling (AAL) template, each of which was considered a node (Behzadi et al. 2007; Whitfield-Gabrieli and Nieto-Castanon 2012). The brain's functional connectivity between two nodes could be represented as an edge. The degree of a node is the number of edges connecting it to the rest of the network, which allows characterizing the edge distribution of all nodes in the network (Bullmore and Bassett 2011).

The resting-state functional image was registered to the T1-weighted image and then to MNI space. The transformation matrix from the resting space to MNI space was calculated by the transformation matrices created in the two aforementioned register processing steps and was stored for later use. We spatially normalized the resting-state functional images to the AAL template in MNI native space, and the connectivity matrix was obtained after functional connectivity analysis. The functional connectivity matrix was acquired from the functional connectivity toolbox (CONN, Neuroimaging Informatics Tools and Resources Clearinghouse, NITRC). Finally, we used the connectivity matrix to perform a graph theoretical analysis.

Analyses of network properties were performed using the Graph Analysis Toolbox (GAT, Stanford University School of Medicine, Stanford, CA, USA) (Hosseini et al. 2012). Previous analysis produced a 90×90 association

connectivity matrix for each individual. GAT extracted the regional mean time series of each of the 90 ROIs, and partial correlation was used to construct undirected weighted networks. Before statistical analyses, the density range in which a network comparison is meaningful needs to be identified (i.e., the density range in which the networks are not fragmented) (Hosseini et al. 2012). After all of the networks were examined, the minimum network density at which no individual network was fragmented was identified as 0.16. The maximum density of the network was determined by the percent of connections present using the most lenient threshold applied, which was 0.5. Next, the networks of the two groups were created at different correlation thresholds, ranging from 0.16 to 0.5, in 0.01 increments. The topological parameters of the brain network were also calculated using graph theoretical analysis, including clustering coefficient (C), normalized clustering coefficient (γ), local efficiency (E_{local}), characteristic path length (L), normalized characteristic path length (λ), global efficiency (E_{global}), small-worldness (σ), and transitivity. To determine the statistically significant differences between the groups in the network topology and regional network measurements, we manually extracted the area under the curve between 0.16 and 0.5 of the density to calculate the p value of the two-sample t test.

Network-based statistical analysis

NBS analysis was used to identify the significance of any connected subnetworks evident in the set of altered connections found in BQ chewers. NBS analysis tries to identify any potentially connected structures formed by an appropriately chosen set of suprathreshold links. The topological extent of any such structure is then used to determine its significance. The test statistic (i.e., primary threshold) computed for each pairwise association is used to construct a set of suprathreshold links (Zalesky et al. 2010). The null distribution of the number of edges was empirically obtained using nonparametric permutation (5000 permutations) to assess the significance of each of the connected edges.

Results

Participants

Table 1 shows the demographic characteristics. There were significant differences in age, years of education, and BNDS scores among the three groups. Therefore, age and years of education were used as covariates for subsequent analysis. There were no significant differences in FTND or AUDIT between the BQ chewers and the TA controls.

FC and SCA

In FC analysis between the BQ chewers and the HC, we found higher FC of the right precuneus (Fig. 1a) and the left precuneus (Fig. 1b) in the BQ chewers, and lower FC of the right insula in the BQ chewers compared with the HC (Fig. 1c, $p < 0.05$). In FC analysis between the BQ chewers and the TA controls, we found higher FC of the right hippocampus in the BQ chewers (Fig. 1d) and lower FC of the right insula (Fig. 1e) and left insula (Fig. 1f) in the BQ chewers compared with the TA controls ($p < 0.05$). In FC analysis between the TA controls and the HC, we found higher FC of the right precuneus (Fig. 1g) and the left precuneus (Fig. 1h) in the TA controls compared with the HC ($p < 0.05$).

Voxel-based analysis (VBA) of mfALFF and mReHo

In VBA analysis of mfALFF between the BQ chewers and the HC (Fig. 2a), we found higher mfALFF activation of the left cuneus and precuneus in the BQ chewers compared with the HC (Fig. 2b, $p < 0.05$ with FDR correction). In VBA analysis of mReHo between the BQ chewers and the HC (Fig. 2c), higher regional homogeneity of the right caudate and right ACC was found in the BQ chewers compared with the HC (Fig. 2d, $p < 0.05$ with FDR correction).

In VBA analysis of mfALFF between the TA controls and the BQ chewers (Fig. 3a), we found higher mfALFF activation of the right fusiform in the BQ chewers compared with the TA controls (Fig. 3b, $p < 0.05$ with FDR correction). In VBA analysis of mReHo between the TA controls and the BQ chewers (Fig. 3c), we found higher regional homogeneity of the left amygdala, left pallidum, left hippocampus, left putamen, left middle frontal gyrus (MFG), left and right superior frontal gyri (SFG), left ACC, and right precuneus in the BQ chewers compared with the TA controls (Fig. 3d, $p < 0.05$ with FDR correction). We also found lower regional homogeneity of the right superior temporal gyrus (STG) in the BQ chewers compared with the TA controls (Fig. 3d, $p < 0.05$ with FDR correction).

In VBA analysis of mfALFF between the TA controls and the HC (Fig. 4a), we found higher mfALFF activation of the left calcarine in the TA controls compared with the HC (Fig. 4b, $p < 0.05$ with FDR correction). In VBA analysis of mReHo between the TA controls and the HC (Fig. 4c), higher regional homogeneity of the right insula was found in the TA controls compared with the HC (Fig. 4d, $p < 0.05$ with FDR correction).

Graph theoretical analysis

In the GTA among the three groups, i.e., BQ chewers, TA controls and HC, we found a significant tendency in the clustering coefficient (Fig. 5a, TA > HC > BQ), local efficiency

Table 1 Demographic and clinical characteristics. Standard deviations are in parentheses

	Betel-quid chewers (BQ) ($n = 16$)		Tobacco- and alcohol-user controls (TA) ($n = 15$)		Healthy controls (HC) ($n = 17$)		F	p
	Mean	(SD)	Mean	(SD)	Mean	(SD)		
Age	37.1	(10.4)	30.1	(4.9)	31.6	(3.6)	$F(2,45) = 4.502$	0.017
Education Years	13.6	(2.1)	15.5	(1.9)	15.8	(2.3)	$F(2,45) = 4.771$	0.013
BNDS	28.4	(3.2)	11.0		11.0		$F(2,44) = 444.311$	<0.001
FTND	4.7	(2.5)	4.2	(2.0)	n / a		$F(1,26) = 0.343$	0.563
AUDIT	10.9	(6.5)	8.1	(7.5)	n / a		$F(1,26) = 1.168$	0.290
Months	173.5	(151.9)	n / a		n / a			
Days	4.8	(2.3)	n / a		n / a			
Number of BQ	20.8	(26.1)	n / a		n / a			

BNDS, Betel-Nut-Dependency Scale; FTND, Fagerstrom Test for Nicotine Dependence; AUDIT, Alcohol Use Disorders Identification Test; months, the average months of chewing BQ; days, the average number of days per week on which chewing occurred; number of BQ, the average number of BQ chewed per day

(Fig. 5b, TA > HC > BQ), and transitivity (Fig. 5c, TA > HC > BQ). However, no significant tendency was found in the characteristic path length (Fig. 5d), normalized characteristic path length (λ) (Fig. 5e), small-worldness (σ) (Fig. 5f), or other topological parameters. Although all participants maintained the small-worldness functional brain network according to the σ calculation, the network was more like a random network in the BQ chewers.

Network-based statistical analysis

In NBS analysis, we compared the edges of the brain networks between the BQ chewers and the HC. More edges in two subnetworks were found in the HC compared with the BQ chewers ($p < 0.05$). The first subnetwork (Fig. 6a) included the connections from the right SFG to the right MFG, right superior orbital frontal gyrus (OFG) to right middle OFG, right MFG to right middle OFG, right SFG to right inferior triangularis frontal gyrus, right SFG to right ACC, right superior OFG to right ACC right middle OFG to right ACC, right inferior triangularis frontal gyrus to left calcarine, left insula to left calcarine, right inferior triangularis frontal gyrus to left lingual gyrus, and left insula to right lingual gyrus.

The second subnetwork (Fig. 6b) included the connections from the left rolandic operculum to the left posterior cingulate cortex (PCC), left rolandic operculum to right PCC, right rolandic operculum to right PCC, left middle cingulate cortex (MCC) to left precuneus, left precuneus to left putamen, left precuneus to right putamen, right precuneus to right putamen, left PCC to left Heschl's gyrus, right PCC to left Heschl's gyrus, left PCC to left superior temporal gyrus (STG), right PCC to left STG, and left precuneus to left STG.

We also compared the edges of the brain networks between the BQ chewers and the TA controls. One subnetwork showed more edges in the TA controls compared with the BQ chewers (Fig. 6c, $p < 0.05$), including the connections from the left gyrus rectus to the left insula, right rolandic operculum to right PCC, left gyrus rectus to right amygdala, left rolandic operculum to right precuneus, left gyrus rectus to right putamen, right PCC to right putamen, right precuneus to right putamen, right PCC to left Heschl's gyrus, and right PCC to left STG.

Another subnetwork showed that more edges were found in the BQ chewers compared with the TA controls (Fig. 6d, $p < 0.05$), including the connections from the left SFG to the right MOG, right MOG to left superior parietal gyrus (SPG), left MOG to right SPG, right MOG to right SPG, left SPG to right precuneus, left olfactory to left middle temporal gyrus (MTG), left SFG to right MTG, and left olfactory to right MTG. However, no significant difference was found between the TA and the HC.

Discussion

In the current rs-fMRI study, we investigated the possible alternations of brain functions in the current BQ chewers. Our hypothesis was partially supported. That is, the enhanced reward system for the BQ chewers (e.g., habitual drug-seeking behavior and react inappropriately to the substance cues) was supported; however, their inhibitory control was relatively preserved. In addition, we reported that the BQ chewers may have enhanced visuospatial processing and decreased local segregation. We discussed these findings in terms of different indexes next.

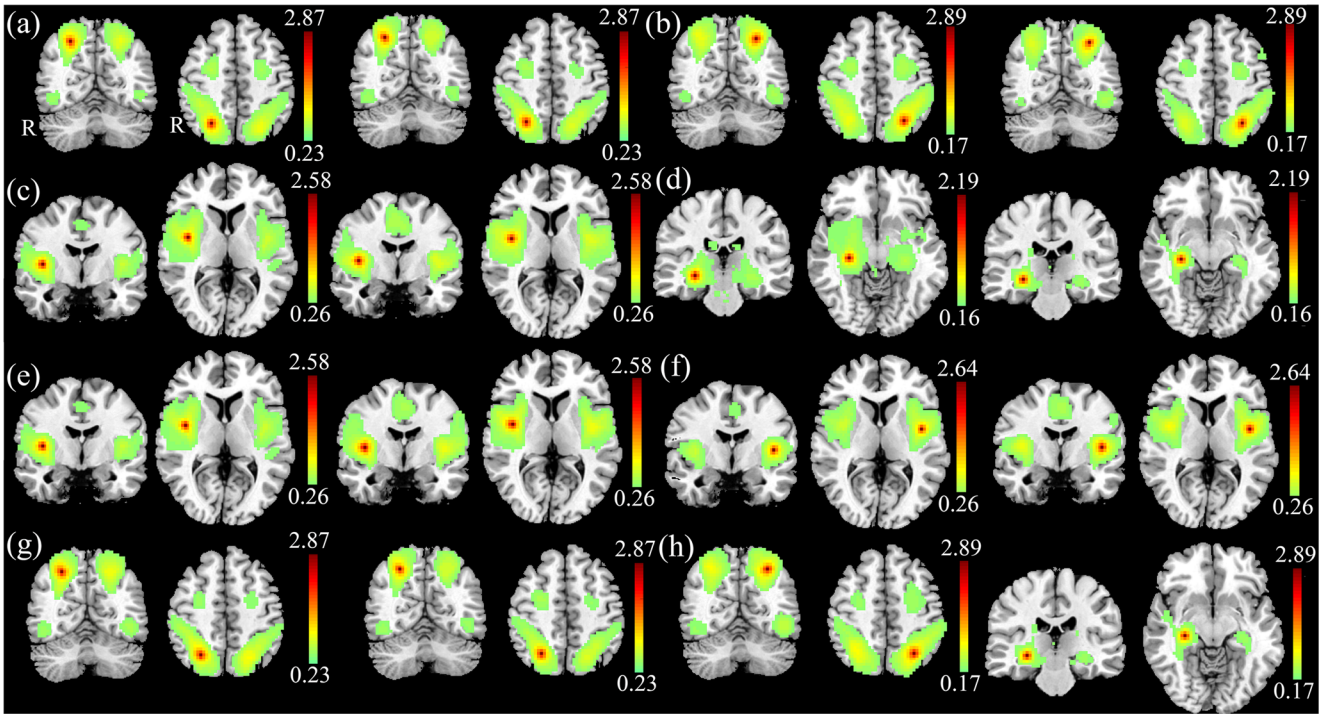

Fig. 1 The higher functional connectivity of (**a**) the right and (**b**) the left precuneus was found in the BQ chewers compared with the HC (left BQ; right HC). (**c**) The lower functional connectivity of the right insula was found in the BQ chewers compared with the HC (left BQ; right HC). (**d**) The higher functional connectivity of the right hippocampus was found in the BQ chewers compared with the TA controls (left BQ; right TA). The lower functional connectivity of (**e**) the right and (**f**) the left insula was found in the BQ chewers compared with the TA controls (left BQ; right TA). The higher functional connectivity of (**g**) the right and (**h**) the left precuneus was found in the TA controls compared with the HC (left TA; right HC)

Functional connectivity: enhanced visuospatial processing, inappropriate reactivity to BQ, possible anti-depressant property

Higher FC of the bilateral precuneus was observed in the BQ chewers (vs. HC) and the TA controls (vs. HC). A recent structural imaging study (Chen et al. 2015) found an increased gray matter (GM) volume of precuneus in BQ chewers. The precuneus is related to identifying the salience of visual, appetitive cues (e.g., BQ for the habitual chewers) (Gearhardt et al. 2014; Tang et al. 2012), suggesting that it plays an important role in visuospatial processing (e.g., directing attention in space and among objects) (Cavanna and Trimble 2006).

Lower FC of the insula was found in the BQ chewers, as compared to the HC and TA controls. Neuroimaging studies have shown that addicted individuals had lower GM volume

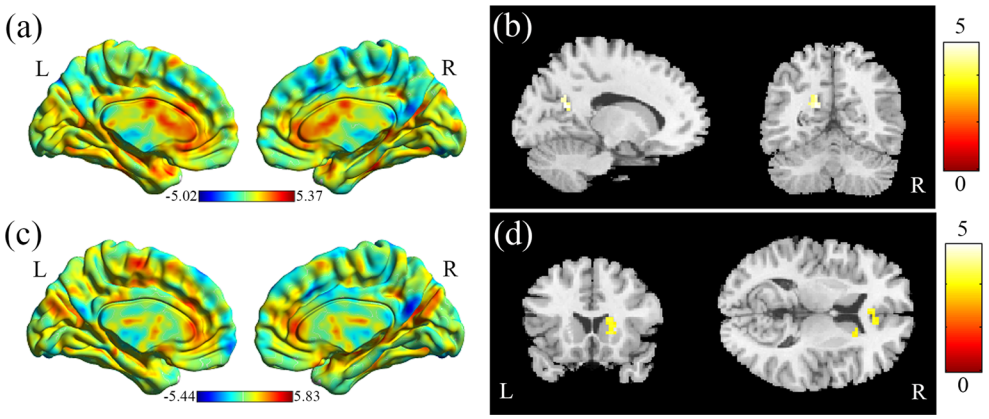

Fig. 2 (**a**) Two-sample *t* test results of mfALFF between the BQ and the HC (BQ > HC; color bar represents *t* score). (**b**) Higher mfALFF of the left cuneus and precuneus was found in the BQ chewers compared with the HC (cluster size = 6, $p < 0.05$ with FDR correction). (**c**) Two-sample *t* test results of mReHo between the BQ and the HC (BQ > HC; color bar represents *t* score). (**d**) Higher mReHo of the right caudate and the right ACC was found in the BQ chewers compared with the HC (cluster size = 22 and 6, $p < 0.05$ with FDR correction)

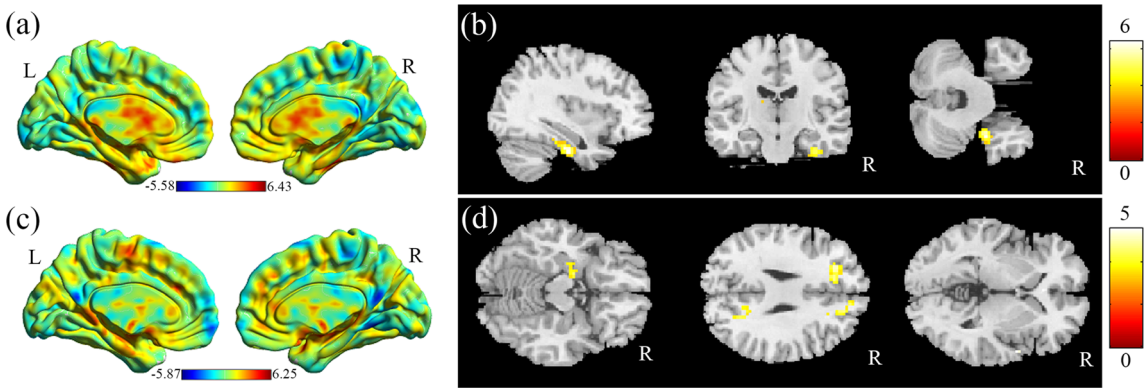

Fig. 3 (**a**) Two-sample *t* test results of mfALFF between the TA and the BQ (TA > BQ; color bar represents *t* score). (**b**) Higher mfALFF was found in the right fusiform in the BQ chewers compared with the TA controls (cluster size = 20, $p < 0.05$ with FDR correction). (**c**) Two-sample *t* test results of mReHo between the TA and the BQ (TA > BQ, color bar represents *t* score). (**d**) Higher mReHo of the left amygdala, the left pallidum, the left hippocampus, and the left putamen was found in the BQ chewers compared with the TA controls (cluster size = 50, $p < 0.05$ with FDR correction). Higher mReHo of the left MFG, left and right SFG, left ACC, and right precuneus was also found in the BQ chewers compared with the TA controls (cluster size = 50, $p < 0.05$ with FDR correction). Lower mReHo of the right STG was found in the BQ chewers compared with the TA controls (cluster size = 5, $p < 0.05$ with FDR correction)

of insula and reduced activity of the insula (Droutman et al. 2015). The insula has a critical role in generating conscious, interoceptive experiences (McClernon et al. 2009; Verdejo-Garcia et al. 2012). A desensitized interoceptive insula in BQ chewers may make them misadjust the reward value of the substance to optimize their choices to satisfy their internal and external need (Naqvi and Bechara 2010; Paulus and Stewart 2014). Another possibility is that the insula and the ACC form a salience network (Menon 2015) that is responsible for detecting the salient event (e.g., BQ for the chewers) and initiating the network switch between the default mode and the central executive networks (Menon and Uddin 2010). The weaker FC of the insula in the BQ chewers may suggest an inappropriate reactivity to salient stimuli, followed by enhanced impulsive substance use and/or decreased engagement of the central executive system (Bechara 2005).

Higher FC of the right hippocampus was found in the BQ chewers, compared to the TA controls. A recent structural imaging study (Chen et al. 2015) also reported increased GM volume of the hippocampus in the BQ chewers. The hippocampus is involved in memory and emotion (Phelps 2004). For example, the intake of arecoline (a primary ingredient in BQ) has been shown to have an acute effect on improving memory (e.g., verbal memory) in patients with Alzheimer's disease (Asthana et al. 1995; Raffaele et al. 1996). However, a recent behavioral study (Chiu et al. 2016) reported impaired spatial short-term memory in dependent BQ chewers. *Areca catechu* fruit extract has been shown to increase serotonin and noradrenaline levels (Abbas et al. 2013), suggesting a possible anti-depressant property. Since the hippocampus is related to emotion, particularly depression (Videbech and Ravnkilde 2004), the stronger FC in the

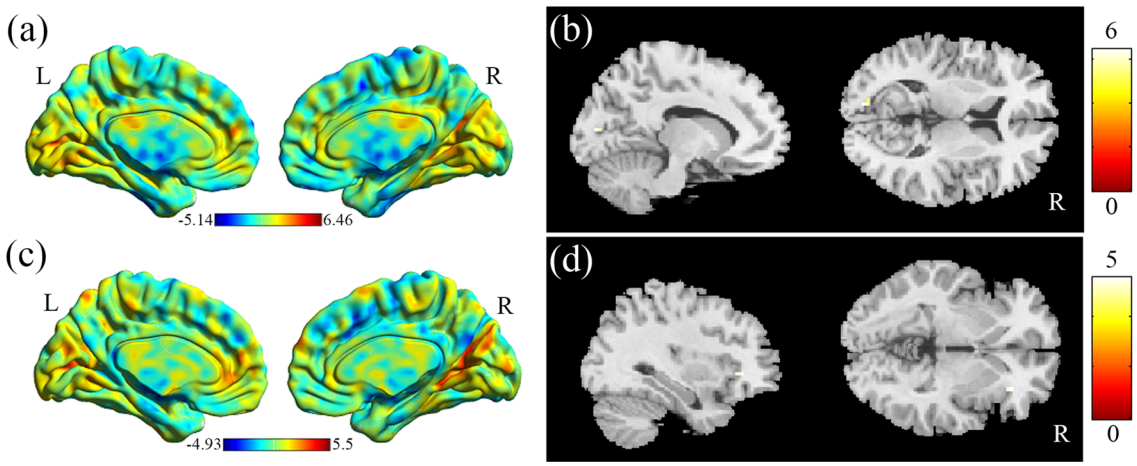

Fig. 4 (**a**) Two-sample *t* test results of mfALFF between the TA and the HC (TA > HC, color bar represents *t* score). (**b**) Higher mfALFF of the left calcarine was found in the TA controls compared with the HC (cluster size = 3, $p < 0.05$ with FDR correction). (**c**) Two-sample *t* test results of mReHo between the TA and the HC (TA > HC, color bar represents *t* score). (**d**) Higher mReHo of the right insula was found in the TA controls compared with the HC (cluster size = 2, $p < 0.05$ with FDR correction)

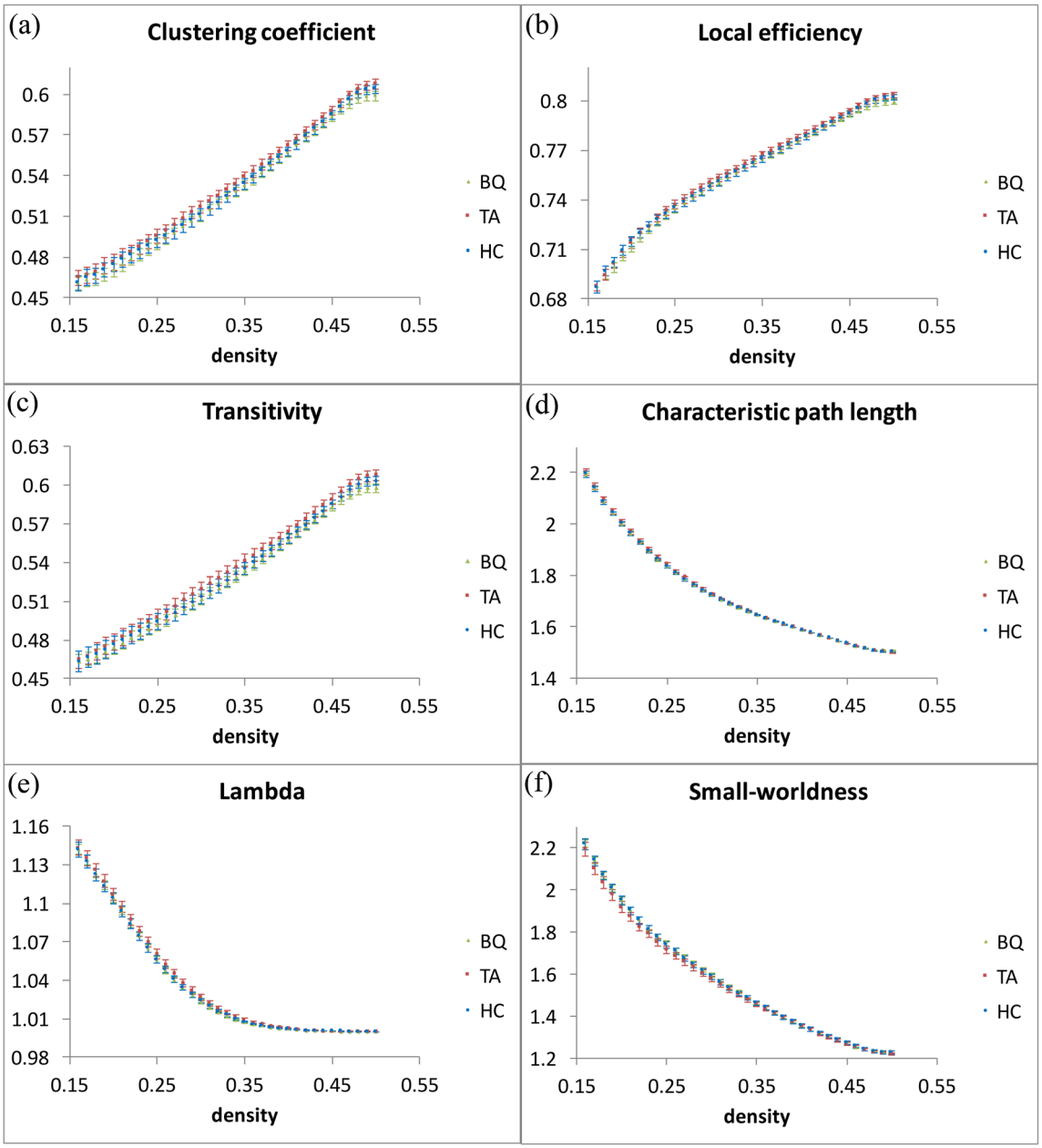

Fig. 5 The topological parameters, including (**a**) clustering coefficient, (**b**) local efficiency, (**c**) transitivity, (**d**) characteristic path length, (**e**) normalized characteristic path length (λ), and (**f**) small-worldness (σ), among the three groups, i.e., the BQ chewers, the TA controls, and the HC

hippocampus in BQ chewers may be a possible neural mechanism underlying the anti-depressant property.

mfALFF: enhanced basic visual processing

Higher mfALFF activation of the left cuneus and precuneus was found in the BQ chewers compared with the HC. The cuneus is important for basic visual processing (e.g., texture and orientation) projected from the retinas. None of the BQ imaging studies reported the enhanced basic visual processing in the BQ chewers. It is possible that repeated addictive substance use may result in the brain's hypersensitivity to the substance and substance-related cues (Ho et al. 2013; Robinson and Berridge 2003; Shen et al. 2016). Future studies are needed to examine the hypothesis of enhanced visual processing.

mReHo: enhanced reward system, preserved attentional control

Higher mReHo activation of the right caudate nucleus and the right ACC was found in the BQ chewers compared with the HC. The dorsal striatum (including the caudate nucleus) in the basal forebrain system has also been

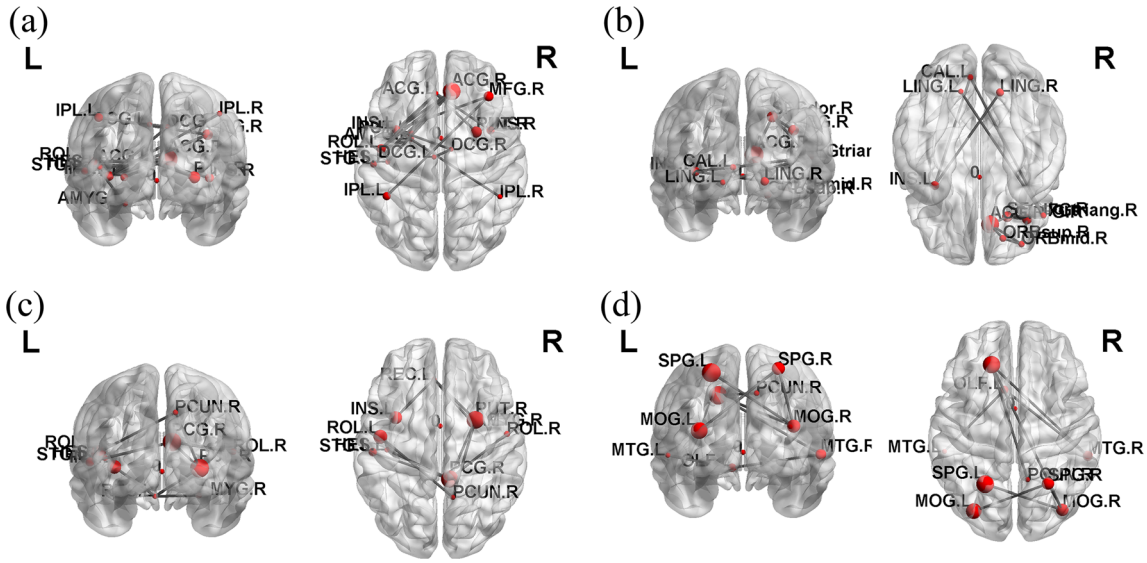

Fig. 6 The NBS results. Two disrupted subnetworks (**a**) and (**b**) were found in the BQ chewers compared with the HC (HC > BQ, $p < 0.05$). (**c**) A disrupted subnetwork was found in the BQ chewers compared with the TA controls (TA > BQ, $p < 0.05$). (**d**) An alternative subnetwork was found in the BQ chewers compared with the TA controls (BQ > TA, $p < 0.05$)

reported to relate to substance cue reactivity (Chase et al. 2011; Jasinska et al. 2014; Kühn and Gallinat 2011). It also plays an important role in habitual drug seeking and in reinforcing learning (Koob and Volkow 2010). The ACC is believed to play a role in inhibitory control over the amygdala-striatal reward system (Ersche et al. 2013; Koob 2006; Volkow et al. 2012). Recent BQ imaging studies appear to have inconsistent results. Some have reported impairment of the ACC in BQ chewers manifested in forms such as decreased GM volume (Chen et al. 2015) and decreased spontaneous brain activity (Liu et al. 2016b), showing impaired inhibitory control. On the other hand, Weng et al. (2017) reported increased diffusion anisotropy in the ACC, possibly showing facilitated inhibitory control in the BQ chewers. A recent behavioral study by Ho et al. (2015) reported that acute and chronic BQ chewing did not affect BQ chewers' inhibitory control (Ho et al. 2015). It is possible that BQ is a weakly addictive substance and that current BQ chewers may not develop dependence symptoms in terms of DSM-IV or ICD-10 (Benegal et al. 2008; Lee et al. 2014).

The BQ chewers had higher mReHo activations in the left putamen, the left amygdala, the left hippocampus, the left pallidum, the left MFG, the left and right SFG, the left ACC, and the right precuneus as compared to the TA controls. The dorsal striatum (putamen and caudate nucleus) and the amygdala are parts of the basal forebrain reward system (Chase et al. 2011; Jasinska et al. 2014; Kühn and Gallinat 2011). The dorsal striatum plays an important role in habitual drug seeking and in reinforcing learning (Koob and Volkow 2010). The amygdala mediates cue-induced reinstatement of drug-seeking behavior (Everitt et al. 2000; See et al. 2003) and promotes negative reinforcement associated with compulsive drug use (Koob and Volkow 2010). The processing of contextual information by the hippocampus and reinforcement by the amygdala together contribute to the preoccupation with substance use (Koob and Volkow 2010). The pallidum in the basal ganglia receives projections primarily from the striatum; therefore it is critical for further processing of the drug reward signal (Koob and Volkow 2010). The BQ chewers may experience the enhanced basal forebrain reward system. This result is consistent with many recent BQ imaging studies (Chen et al. 2015; Liu et al. 2016a; Weng et al. 2017).

The ACC, MFG, and SFG are involved in attentional control. As mentioned earlier, the ACC plays an important role in inhibitory control. The MFG is involved in reorienting attention from stimulus-driven, exogenous attention to top-down guided endogenous attentional control (Chica et al. 2013; Japee et al. 2015). Chen et al. (2015) reported that a longer period of BQ chewing is related to a larger reduction of GM of MFG (Chen et al. 2015). However, Chen et al. did not report a significant between-group GM difference in MFG. The SFG supports working memory and top-down attentional orienting (Du Boisgueheneuc et al. 2006; Hopfinger et al. 2000). A recent structural imaging study reported decreased diffusion anisotropy in the bilateral SFG in BQ chewers (Weng et al. 2017). The current rs-fMRI study reported the possible enhancement of attentional control in the BQ chewers; however, the structural imaging studies (Chen et al. 2015; Weng et al. 2017) may suggest structural abnormalities in the BQ chewers.

The BQ chewers had lower mReHo activations in the right STG as compared to the TA controls. Chen et al. (2015) reported atrophy in the right STG in the BQ chewers, but Liu

et al. (2016b) reported increased neural synchronization in this area. A recent meta-analytic paper (Ersche et al. 2013) suggested that the pattern of reduced volume of STG is not strongly reported in chronic cocaine and amphetamine users. The STG has been involved in auditory processing (Moerel et al. 2014), perception of facial emotions (Bigler et al. 2007), and social cognition (Jou et al. 2010). Liu et al. (2016b) argued that the increased activity in the temporal regions (including the STG) may be a positive reinforcement factor for developing repetitive BQ chewing behavior. More imaging studies on BQ chewers are needed to clarify the role of the STG in BQ chewers and in their development of addiction.

The TA controls had higher mReHo activations in the right insula than the HC. This finding of increased mReHo in the insula is consistent with imaging studies that recruited smokers (Yu et al. 2013) and alcoholic drinkers (Kim et al. 2015). The enhanced synchronization in local regional activity in the insula in TA controls may reflect an atypical urge to use cigarettes and alcohol (Naqvi et al. 2007). On the other hand, however, structural imaging studies showed reduced GM volume of the insula in the addicted individuals (Droutman et al. 2015). Similarly, functional imaging studies showed weaker FC of the insula in opioid (Upadhyay et al. 2010) and cocaine (Gu et al. 2010) users. Alternatively, task-based functional imaging studies showed mixed results; that is, reduced insular activity in the decision-making task and the cue-reactivity task, but increased activity in the Go/No-Go task. More task-based imaging studies are needed to understand the role of the insula in addiction (Droutman et al. 2015).

GTA: decreased local segregation

In the graph theoretical analysis, we reported that the TA controls had the largest clustering coefficient, local efficiency, and transitivity whereas the BQ chewers had the lowest (i.e., TA > HC > BQ). The current results suggest that the BQ chewers may have worse segregated neural processing (lower clustering coefficient, local efficiency, and transitivity), as compared to the HC and TA controls. Alternatively, the TA controls have better segregated neutral processing than the HC and BQ chewers.

The clustering coefficient quantifies the extent of local interconnectivity in the network. The local efficiency indicates how well a node exchanges information with its immediate neighbors. The transitivity refers to the extent to which the relation between two nodes in a network that are connected by an edge is transitive. These measures reflect the extent of local segregation of the neural network: higher scores on these measures correspond to a higher extent of segregated neural processing (e.g., higher local interconnectivity, higher efficiency of local information exchanges, and higher transitivity between nodes). On the other hand, the three groups exhibit small-world properties (σ) and have a similar extent of global integration of the neural network (e.g., characteristic path length and normalized characteristic path length). The three groups exhibit small-world properties, suggesting a balance between local segregation and global integration among the brain regions and networks (Bullmore and Bassett 2011; Hosseini et al. 2012). Path length is defined as the minimum number of edges between all pairs of nodes (Bullmore and Bassett 2011; Hosseini et al. 2012). Increased path length indicates decreased global integration of the network. The three groups have a similar extent of global integration. We suggest that the BQ chewers have decreased local segregation and relatively intact global integration, which may lead to a reduction in the specificity with which distinct neural structures mediate particular processing functions (e.g., long-term memory) (Chan et al. 2014).

NBS analysis: disrupted subnetwork of the control system and DMN and facilitated subnetwork of visuospatial processing

The BQ chewers had two disrupted subnetworks (Fig. 6a, b) in comparison to the HC (HC > BQ) and one disrupted subnetwork (Fig. 6c) compared to the TA controls (TA > BQ). Alternatively, the BQ chewers had one enhanced subnetwork (Fig. 6d) as compared to the TA controls (BQ > TA).

The first disrupted subnetwork (HC > BQ, Fig. 6a) may involve primarily the brain areas playing important roles in the control system and in decision-making. For example, the OFG integrates the emotional/somatic states and working memory for decision making (Li et al. 2010). The ACC is believed to play a role in inhibitory control over the amygdala–striatal reward system (Ersche et al. 2013; Koob 2006; Volkow et al. 2012). The SFG supports working memory and top-down attentional orienting (Du Boisgueheneuc et al. 2006; Hopfinger et al. 2000).

The second disrupted subnetwork (HC > BQ, Fig. 6b) may involve primarily the brain areas in the DMN (e.g., the precuneus and the PCC) (Fransson and Marrelec 2008). Liu et al. found that the BQ chewers had decreased connectivity from the ACC to the DMN (Liu et al. 2016a). The disrupted DMN may impair the chewers' awareness of disease, their need for treatment, and/or their strong desire for the drug (Buckner et al. 2008; Goldstein et al. 2009; Volkow et al. 2012).

The third disrupted subnetwork (TA > BQ, Fig. 6c) involves primarily the DMN and the amygdala-striatal reward system (e.g., the putamen and amygdala). The dorsal striatum (including the putamen) plays an important role in habitual drug seeking and in reinforcing learning (Koob and Volkow 2010). The amygdala mediates the cue-induced reinstatement of drug-seeking behavior (Everitt et al. 2000; See et al. 2003) and promotes negative reinforcement associated with compulsive drug use (Koob and Volkow 2010). The reductions of resting-state connectivity in these areas may

reflect a possible difficulty in appropriately engaging the circuitry associated with reward, motivation, and emotion, such as decreased reward systems driven by natural rewards (Koob and Le Moal 2005; Sutherland et al. 2012).

The only enhanced subnetwork (BQ > TA, Fig. 6d) involves primarily visual (e.g., the MOG) and spatial processing (e.g., the SPG). The MOG is primarily involved in the spatial and nonspatial processing of visual stimuli (Renier et al. 2010). The SPG is primarily involved in spatial attention and perception (Cabeza and Nyberg 2000). This result is similar to the recent finding (Huang et al. 2016), showing that acute BQ chewing can increase new participants' visuospatial processing. Previous behavioral studies (Ho and Wang 2010, 2011) also reported that BQ chewing can immediately facilitate the habitual chewers' visuospatial processing (e.g., making it easier to detect a parafoveal target).

Conclusions

In this study, we used rs-fMRI to examine the brain functional alterations in BQ chewers compared to the TA controls and the HC. The data were analyzed by FC, mfALFF, mReHo, GTA, and NBS analyses. To summarize, we report that the BQ chewers may have inappropriate reactivity to BQ, an enhanced reward system, preserved attentional control, enhanced visuospatial processing, and decreased local segregation. In the future, the task-based fMRI studies are encouraged for better understanding of higher-level functional changes (e.g., attentional control) for the chronic BQ chewers. This study was limited in relatively small sample size, which may affect the significance and possibly bias the results.

Acknowledgements The authors would like to thank Jau-Yang Lin for his assistance in experimental preparation.

Funding information This study was supported by the research programs NSC103-2420-H-040-001-MY2, MOST105-2410-H-040-001-MY3, and MOST106-2221-E-182-079, which were sponsored by the Ministry of Science and Technology, Taipei, Taiwan.

Compliance with ethical standards

Conflict of interest The authors declare that they have no conflict of interest.

References

Abbas G, Naqvi S, Erum S, Ahmed S, Dar A (2013) Potential antidepressant activity of Areca catechu nut via elevation of serotonin and noradrenaline in the hippocampus of rats. Phytother Res 27:39–45

Asthana S, Raffaele KC, Greig NH, Berardi A, Morris PP, Schapiro MB, Rapoport SI, Blackman MR, Soncrant TT (1995) Neuroendocrine responses to intravenous infusion of arecoline in patients with Alzheimer's disease. Psychoneuroendocrinology 20(6):623–636. https://doi.org/10.1016/0306-4530(94)00084-N

Baria AT, Baliki MN, Parrish T, Apkarian AV (2011) Anatomical and functional assemblies of brain BOLD oscillations. J Neurosci 31(21):7910–7919. https://doi.org/10.1523/JNEUROSCI.1296-11.2011

Bechara A (2005) Decision making, impulse control and loss of willpower to resist drugs: a neurocognitive perspective. Nat Neurosci 8(11):1458–1463. https://doi.org/10.1038/nn1584

Behzadi Y, Restom K, Liau J, Liu TT (2007) A component based noise correction method (CompCor) for BOLD and perfusion based fMRI. NeuroImage 37(1):90–101. https://doi.org/10.1016/j.neuroimage.2007.04.042

Benegal V, Rajkumar RP, Muralidharan K (2008) Does areca nut use lead to dependence? Drug Alcohol Depend 97(1-2):114–121. https://doi.org/10.1016/j.drugalcdep.2008.03.016

Bigler ED, Mortensen S, Neeley ES, Ozonoff S, Krasny L, Johnson M, Lu J, Provencal SL, McMahon W, Lainhart JE (2007) Superior temporal gyrus, language function, and autism. Dev Neuropsychol 31(2):217–238. https://doi.org/10.1080/87565640701190841

Biswal B, Yetkin FZ, Haughton VM, Hyde JS (1995) Functional connectivity in the motor cortex of resting human brain using echo-planar MRI. Magn Reson Med 34(4):537–541. https://doi.org/10.1002/mrm.1910340409

Buckner RL, Andrews-Hanna JR, Schacter DL (2008) The brain's default network. Ann N Y Acad Sci 1124(1):1–38. https://doi.org/10.1196/annals.1440.011

Bullmore ET, Bassett DS (2011) Brain graphs: graphical models of the human brain connectome. Annu Rev Clin Psychol 7(1):113–140. https://doi.org/10.1146/annurev-clinpsy-040510-143934

Bullmore ET, Sporns O (2009) Complex brain networks: graph theoretical analysis of structural and functional systems. Nat Rev Neurosci 10(3):186–198. https://doi.org/10.1038/nrn2575

Cabeza R, Nyberg L (2000) Imaging cognition II: an empirical review of 275 PET and fMRI studies. J Cognit Neurosci 12(1):1–47. https://doi.org/10.1162/08989290051137585

Cavanna AE, Trimble MR (2006) The precuneus: a review of its functional anatomy and behavioural correlates. Brain 129(3):564–583. https://doi.org/10.1093/brain/awl004

Chan MY, Park DC, Savalia NK, Petersen SE, Wig GS (2014) Decreased segregation of brain systems across the healthy adult lifespan. Proc Natl Acad Sci 111(46):E4997–E5006. https://doi.org/10.1073/pnas.1415122111

Chase HW, Eickhoff SB, Laird AR, Hogarth L (2011) The neural basis of drug stimulus processing and craving: an activation likelihood estimation meta-analysis. Biol Psychiatry 70(8):785–793. https://doi.org/10.1016/j.biopsych.2011.05.025

Chen CH, Chen WJ, Cheng AT (2005) New approach to the validity of the alcohol use disorders identification test: stratum-specific likelihood ratios analysis. Alcohol Clin Exp Res 29(4):602–608. https://doi.org/10.1097/01.ALC.0000159189.56671.EC

Chen F, Zhong Y, Zhang Z, Xu Q, Liu T, Pan M, Li J, Lu G (2015) Gray matter abnormalities associated with betel quid dependence: a voxel-based morphometry study. Am J Transl Res 7(2):364–374

Chen VC, Shen CY, Liang SH, Li ZH, Tyan YS, Liao YT, Huang YC, Lee Y, McIntyre RS, Weng JC (2016) Assessment of abnormal brain structures and networks in major depressive disorder using morphometric and connectome analyses. J Affect Disord 205:103–111. https://doi.org/10.1016/j.jad.2016.06.066

Chica AB, Bartolomeo P, Lupiáñez J (2013) Two cognitive and neural systems for endogenous and exogenous spatial attention. Behav Brain Res 237:107–123

Chiu M-C, Shen B, Li S-H, Ho M-C (2016) Spatial short-term memory is impaired in dependent betel quid chewers. Psychopharmacology 233(15-16):2925–2932. https://doi.org/10.1007/s00213-016-4331-9

Cordes D, Haughton VM, Arfanakis K, Carew JD, Turski PA, Moritz CH, Quigley MA, Meyerand ME (2001) Frequencies contributing to functional connectivity in the cerebral cortex in "resting-state" data. AJNR Am J Neuroradiol 22(7):1326–1333

Droutman V, Read SJ, Bechara A (2015) Revisiting the role of the insula in addiction. Trends Cogn Sci 19(7):414–420. https://doi.org/10.1016/j.tics.2015.05.005

Du Boisgueheneuc F, Levy R, Volle E, Seassau M, Duffau H, Kinkingnehun S, Samson Y, Zhang S, Dubois B (2006) Functions of the left superior frontal gyrus in humans: a lesion study. Brain 129:3315–3328

Ersche KD, Jones PS, Williams GB, Turton AJ, Robbins TW, Bullmore ET (2012) Abnormal brain structure implicated in stimulant drug addiction. Science 335(6068):601–604. https://doi.org/10.1126/science.1214463

Ersche KD, Williams GB, Robbins TW, Bullmore ET (2013) Meta-analysis of structural brain abnormalities associated with stimulant drug dependence and neuroimaging of addiction vulnerability and resilience. Curr Opin Neurobiol 23(4):615–624. https://doi.org/10.1016/j.conb.2013.02.017

Everitt BJ, Cardinal RN, Hall J, Parkinson J, & Robbins T (2000) Differential involvement of amygdala subsystems in appetitive conditioning and drug addiction. In: Aggleton JP (ed), The amygdala: a functional analysis, Oxford University Press, Oxford, p 353-390

Fagerström K-O (1978) Measuring degree of physical dependence to tobacco smoking with reference to individualization of treatment. Addict Behav 3(3-4):235–241. https://doi.org/10.1016/0306-4603(78)90024-2

Fransson P, Marrelec G (2008) The precuneus/posterior cingulate cortex plays a pivotal role in the default mode network: evidence from a partial correlation network analysis. NeuroImage 42(3):1178–1184. https://doi.org/10.1016/j.neuroimage.2008.05.059

Gearhardt AN, Yokum S, Stice E, Harris JL, Brownell KD (2014) Relation of obesity to neural activation in response to food commercials. Soc Cogn Affect Neurosci 9(7):932–938. https://doi.org/10.1093/scan/nst059

Goldstein RZ, Bechara A, Garavan H, Childress AR, Paulus MP, Volkow ND (2009) The neurocircuitry of impaired insight in drug addiction. Trends Cogn Sci 13(9):372–380. https://doi.org/10.1016/j.tics.2009.06.004

Gong Q, He Y (2015) Depression, neuroimaging and connectomics: a selective overview. Biol Psychiatry 77(3):223–235. https://doi.org/10.1016/j.biopsych.2014.08.009

Greicius MD, Krasnow B, Reiss AL, Menon V (2003) Functional connectivity in the resting brain: a network analysis of the default mode hypothesis. Proc Natl Acad Sci U S A 100(1):253–258. https://doi.org/10.1073/pnas.0135058100

Gu H, Salmeron BJ, Ross TJ, Geng X, Zhan W, Stein EA, Yang Y (2010) Mesocorticolimbic circuits are impaired in chronic cocaine users as demonstrated by resting-state functional connectivity. NeuroImage 53(2):593–601. https://doi.org/10.1016/j.neuroimage.2010.06.066

Ho MC (2014) Commentary on Lee et al. (2014): betel-quid—when east encounters west. Addiction 109(7):1205–1206. https://doi.org/10.1111/add.12614

Ho MC, Chang CF, Li RH, Tang TC (2013) Attentional biases for betel nut cues in heavy and light chewers. Psychol Addict Behav 27(4):1044–1049. https://doi.org/10.1037/a0030562

Ho MC, Li RH, Tang TC (2015) Betel nut chewing effects on sustained attention and inhibitory control after sleep deprivation. Aust J Psychol 67(4):222–230. https://doi.org/10.1111/ajpy.12081

Ho MC, Wang CK (2010) Can betel nut chewing affect the UFOV size after sleep deprivation? Chin J Psychol 52:445–456

Ho MC, Wang CK (2011) The effect of betel nut chewing on contour and object masking. Atten Percept Psychophys 73(8):2583–2593. https://doi.org/10.3758/s13414-011-0214-7

Hopfinger JB, Buonocore MH, Mangun GR (2000) The neural mechanisms of top-down attentional control. Nat Neurosci 3(3):284–291. https://doi.org/10.1038/72999

Hosseini SM, Hoeft F, Kesler SR (2012) GAT: a graph-theoretical analysis toolbox for analyzing between-group differences in large-scale structural and functional brain networks. PLoS One 7:e40709

Huang C-L, Lin H-H, Wang H-H (2006) The psychometric properties of the Chinese version of the Fagerstrom test for nicotine dependence. Addict Behav 31(12):2324–2327. https://doi.org/10.1016/j.addbeh.2006.02.024

Huang X, Liu Z, Mwansisya TE, Pu W, Zhou L, Liu C, Chen X, Rohrbaugh R, Marienfeld C, Xue Z (2016) Betel quid chewing alters functional connectivity in frontal and default networks: a resting-state fMRI study. J Magn Reson Imaging 45(1):157–166

Huang X, Pu W, Liu H, Li X, Greenshaw AJ, Dursun SM, Xue Z, Liu Z (2017) Altered brain functional connectivity in betel quid-dependent chewers. Front Psych 8:239. https://doi.org/10.3389/fpsyt.2017.00239

IARC (2004) Betel-quid and areca-nut chewing and some areca-nut-derived nitrosamines. IARC Monogr Eval Carcinog Risks Hum, Lyon

Japee S, Holiday K, Satyshur MD, Mukai I, Ungerleider LG (2015) A role of right middle frontal gyrus in reorienting of attention: a case study. Front Syst Neurosci 9:1–16

Jasinska AJ, Stein EA, Kaiser J, Naumer MJ, Yalachkov Y (2014) Factors modulating neural reactivity to drug cues in addiction: a survey of human neuroimaging studies. Neurosci Biobehav Rev 38:1–16. https://doi.org/10.1016/j.neubiorev.2013.10.013

Jou RJ, Minshew NJ, Keshavan MS, Vitale MP, Hardan AY (2010) Enlarged right superior temporal gyrus in children and adolescents with autism. Brain Res 1360:205–212. https://doi.org/10.1016/j.brainres.2010.09.005

Kühn S, Gallinat J (2011) Common biology of craving across legal and illegal drugs—a quantitative meta-analysis of cue-reactivity brain response. Eur J Neurosci 33(7):1318–1326. https://doi.org/10.1111/j.1460-9568.2010.07590.x

Kim H, Kim YK, Gwak AR, Lim J-A, Lee J-Y, Jung HY, Sohn BK, Choi S-W, Choi J-S (2015) Resting-state regional homogeneity as a biological marker for patients with internet gaming disorder: a comparison with patients with alcohol use disorder and healthy controls. Prog Neuro-Psychopharmacol Biol Psychiatry 60:104–111. https://doi.org/10.1016/j.pnpbp.2015.02.004

Ko YC, Chiang TA, Chang SJ, Hsieh SF (1992) Prevalence of betel quid chewing habit in Taiwan and related sociodemographic factors. J Oral Pathol Med 21(6):261–264. https://doi.org/10.1111/j.1600-0714.1992.tb01007.x

Koob GF (2006) The neurobiology of addiction: a neuroadaptational view relevant for diagnosis. Addiction 101:23–30. https://doi.org/10.1111/j.1360-0443.2006.01586.x

Koob GF, Le Moal M (2005) Plasticity of reward neurocircuitry and the 'dark side' of drug addiction. Nat Neurosci 8(11):1442–1444. https://doi.org/10.1038/nn1105-1442

Koob GF, Volkow ND (2010) Neurocircuitry of addiction. Neuropsychopharmacology 35(1):217–238. https://doi.org/10.1038/npp.2009.110

Lee CH, Chiang SL, Ko AMS, Hua CH, Tsai MH, Warnakulasuriya S, Ibrahim SO, Zain RB, Ling TY, Huang CL (2014) Betel-quid dependence domains and syndrome associated with betel-quid ingredients among chewers: an Asian multi-country evidence. Addiction 109(7):1194–1204. https://doi.org/10.1111/add.12530

Li RH, Ho MC, Tang TC, Chang CF (2012) Development of the betel nut dependency scale (BNDS). Chin J Psychol 54:331–348

Li X, Lu ZL, D'Argembeau A, Ng M, Bechara A (2010) The Iowa gambling task in fMRI images. Hum Brain Mapp 31(3):410–423. https://doi.org/10.1002/hbm.20875

Liu T, Li J-j, Zhao Z-g, Zhong Y, Zhang Z-q, Xu Q, Yang G-s, Lu G-m, Pan S-y, Chen F (2016a) Betel quid dependence is associated with functional connectivity changes of the anterior cingulate cortex: a resting-state fMRI study. J Transl Med 14:1. https://doi.org/10.1186/s12967-016-0784-1

Liu T, Li J-j, Zhao Z-y, Yang G-s, Pan M-j, Li C-q, Pan S-y, Chen F (2016b) Altered spontaneous brain activity in betel quid dependence: a resting-state functional magnetic resonance imaging study. Medicine 95(5):e2638

Liu T, Li J, Zhang Z, Xu Q, Lu G, Huang S, Pan M, Chen F (2016c) Altered long-and short-range functional connectivity in patients with betel quid dependence: a resting-state functional MRI study. Cell Physiol Biochem 40(6):1626–1636. https://doi.org/10.1159/000453212

Liu T, Li J, Huang S, Zhao Z, Yang G, Pan M, Li C, Chen F, Pan S (2015) Neurochemical abnormalities in anterior cingulate cortex on betel quid dependence: a 2D 1H MRS investigation. Am J Transl Res 7:2795

Lo CY, He Y, Lin CP (2011) Graph theoretical analysis of human brain structural networks. Rev Neurosci 22:551–563

McClernon FJ, Kozink RV, Lutz AM, Rose JE (2009) 24-h smoking abstinence potentiates fMRI-BOLD activation to smoking cues in cerebral cortex and dorsal striatum. Psychopharmacology 204(1):25–35. https://doi.org/10.1007/s00213-008-1436-9

Menon V (2015) Salience network. Brain Mapp 2:597–611

Menon V, Uddin LQ (2010) Saliency, switching, attention and control: a network model of insula function. Brain Struct Funct 214(5-6):655–667. https://doi.org/10.1007/s00429-010-0262-0

MHW (2008) 905 betel nut chewing. Retrieved from https://www.mohw.gov.tw/dl-37747-2317188e-1f02-407b-a54a-ef4d0f663473.html

Moerel M, De Martino F, Formisano E (2014) An anatomical and functional topography of human auditory cortical areas. Front Neurosci 8:225

Naqvi NH, Bechara A (2010) The insula and drug addiction: an interoceptive view of pleasure, urges, and decision-making. Brain Struct Funct 214(5-6):435–450. https://doi.org/10.1007/s00429-010-0268-7

Naqvi NH, Rudrauf D, Damasio H, Bechara A (2007) Damage to the insula disrupts addiction to cigarette smoking. Science 315(5811):531–534. https://doi.org/10.1126/science.1135926

Osborne PG, Ko Y-C, Wu M-T, Lee C-H (2017) Intoxication and substance use disorder to Areca catechu nut containing betel quid: a review of epidemiological evidence, pharmacological basis and social factors influencing quitting strategies. Drug Alcohol Depend 179:187–197. https://doi.org/10.1016/j.drugalcdep.2017.06.039

Paulus MP, Stewart JL (2014) Interoception and drug addiction. Neuropharmacology 76:342–350. https://doi.org/10.1016/j.neuropharm.2013.07.002

Phelps EA (2004) Human emotion and memory: interactions of the amygdala and hippocampal complex. Curr Opin Neurobiol 14(2):198–202. https://doi.org/10.1016/j.conb.2004.03.015

Philip NS, Kuras YI, Valentine TR, Sweet LH, Tyrka AR, Price LH, Carpenter LL (2013) Regional homogeneity and resting state functional connectivity: associations with exposure to early life stress. Psychiatry Res 214(3):247–253. https://doi.org/10.1016/j.pscychresns.2013.07.013

Raffaele KC, Asthana S, Berardi A, Haxby JV, Morris PP, Schapiro MB, Soncrant TT (1996) Differential response to the cholinergic agonist arecoline among different cognitive modalities in Alzheimer's disease. Neuropsychopharmacology 15(2):163–170. https://doi.org/10.1016/0893-133X(95)00179-H

Raichle ME, MacLeod AM, Snyder AZ, Powers WJ, Gusnard DA, Shulman GL (2001) A default mode of brain function. Proc Natl Acad Sci U S A 98(2):676–682. https://doi.org/10.1073/pnas.98.2.676

Renier LA, Anurova I, De Volder AG, Carlson S, VanMeter J, Rauschecker JP (2010) Preserved functional specialization for spatial processing in the middle occipital gyrus of the early blind. Neuron 68(1):138–148. https://doi.org/10.1016/j.neuron.2010.09.021

Robinson TE, Berridge KC (2003) Addiction. Annu Rev Psychol 54(1):25–53. https://doi.org/10.1146/annurev.psych.54.101601.145237

Saunders JB, Aasland OG, Babor TF, Grant M (1993) Development of the alcohol use disorders identification test (AUDIT): WHO collaborative project on early detection of persons with harmful alcohol consumption—II. Addiction 88(6):791–804. https://doi.org/10.1111/j.1360-0443.1993.tb02093.x

See RE, Fuchs RA, Ledford CC, McLaughlin J (2003) Drug addiction, relapse, and the amygdala. Ann N Y Acad Sci 985:294–307

Shen B, Chiu M-C, Li S-H, Huang G-J, Liu L-J, Ho M-C (2016) Attentional bias to betel quid cues: an eye tracking study. Psychol Addict Behav 30(6):705–711. https://doi.org/10.1037/adb0000191

Sutherland MT, McHugh MJ, Pariyadath V, Stein EA (2012) Resting state functional connectivity in addiction: lessons learned and a road ahead. NeuroImage 62(4):2281–2295. https://doi.org/10.1016/j.neuroimage.2012.01.117

Tang D, Fellows L, Small D, Dagher A (2012) Food and drug cues activate similar brain regions: a meta-analysis of functional MRI studies. Physiol Behav 106(3):317–324. https://doi.org/10.1016/j.physbeh.2012.03.009

Upadhyay J, Maleki N, Potter J, Elman I, Rudrauf D, Knudsen J, Wallin D, Pendse G, McDonald L, Griffin M, Anderson J, Nutile L, Renshaw P, Weiss R, Becerra L, Borsook D (2010) Alterations in brain structure and functional connectivity in prescription opioid-dependent patients. Brain 133(7):2098–2114. https://doi.org/10.1093/brain/awq138

Verdejo-Garcia A, Clark L, Dunn BD (2012) The role of interoception in addiction: a critical review. Neurosci Biobehav Rev 36(8):1857–1869. https://doi.org/10.1016/j.neubiorev.2012.05.007

Videbech P, Ravnkilde B (2004) Hippocampal volume and depression: a meta-analysis of MRI studies. Am J Psychiatry 161(11):1957–1966. https://doi.org/10.1176/appi.ajp.161.11.1957

Volkow ND, Wang G-J, Fowler JS, Tomasi D (2012) Addiction circuitry in the human brain. Annu Rev Pharmacol Toxicol 52(1):321–336. https://doi.org/10.1146/annurev-pharmtox-010611-134625

Wen C, Tsai S, Cheng T, Chen C, Levy D, Yang H, Eriksen M (2005) Uncovering the relation between betel quid chewing and cigarette smoking in Taiwan. Tob Control 14:i16–i22

Weng J-C, Kao T-W, Huang G-J, Tyan Y-S, Tseng H-C, Ho M-C (2017) Evaluation of structural connectivity changes in betel-quid chewers using generalized q-sampling MRI. Psychopharmacology 234(13):1945–1955. https://doi.org/10.1007/s00213-017-4602-0

Whitfield-Gabrieli S, Nieto-Castanon A (2012) Conn: a functional connectivity toolbox for correlated and anticorrelated brain networks. Brain Connect 2(3):125–141. https://doi.org/10.1089/brain.2012.0073

Winstock AR (2002) Areca nut—abuse liability, dependence and public health. Addict Biol 7(1):133–138. https://doi.org/10.1080/13556210120091509

Yu R, Zhao L, Tian J, Qin W, Wang W, Yuan K, Li Q, Lu L (2013) Regional homogeneity changes in heavy male smokers: a resting-state functional magnetic resonance imaging study. Addict Biol 18(4):729–731. https://doi.org/10.1111/j.1369-1600.2011.00359.x

Yuan F, Kong L, Zhu X, Jiang C, Fang C, Liao W (2017) Altered gray-matter volumes associated with betel quid dependence. Front Psych 8:139

Yue Y, Jia X, Hou Z, Zang Y, Yuan Y (2015) Frequency-dependent amplitude alterations of resting-state spontaneous fluctuations in late-onset depression. Biomed Res Int 2015:505479

Zalesky A, Fornito A, Bullmore ET (2010) Network-based statistic: identifying differences in brain networks. NeuroImage 53:1197–1207

Zang Y, Jiang T, Lu Y, He Y, Tian L (2004) Regional homogeneity approach to fMRI data analysis. NeuroImage 22(1):394–400. https://doi.org/10.1016/j.neuroimage.2003.12.030

Zhang J, Wang J, Wu Q, Kuang W, Huang X, He Y, Gong Q (2011) Disrupted brain connectivity networks in drug-naive, first-episode major depressive disorder. Biol Psychiatry 70(4):334–342. https://doi.org/10.1016/j.biopsych.2011.05.018

Zhang X, Zhu X, Wang X, Zhu X, Zhong M, Yi J, Rao H, Yao S (2014) First-episode medication-naive major depressive disorder is associated with altered resting brain function in the affective network. PLoS One 9(1):e85241. https://doi.org/10.1371/journal.pone.0085241

Zhu X, Zhu Q, Jiang C, Shen H, Wang F, Liao W, Yuan F (2017) Disrupted resting-state default mode network in betel quid-dependent individuals. Front Psychol 8:84. https://doi.org/10.3389/fpsyg.2017.00084

Zou QH, Zhu CZ, Yang Y, Zuo XN, Long XY, Cao QJ, Wang YF, Zang YF (2008) An improved approach to detection of amplitude of low-frequency fluctuation (ALFF) for resting-state fMRI: fractional ALFF. J Neurosci Methods 172(1):137–141. https://doi.org/10.1016/j.jneumeth.2008.04.012